Research Paper

Aloe vera Nanoparticles Loaded with Antihypertensive Beta-Blockers of Different Half-Life: Entrapment Efficiency and Release Behavior

RACHANA SHARMA[1]*, UMA SHARMA AND S. K. PASWAN[2]

School of Studies in Chemistry and Biochemistry, Vikram University, Ujjain, Madhya Pradesh 456010, [1]Parul Institute of Applied Sciences, Parul University, Vadodara, Gujarat 391760, [2]Department of Pharmacy, Industrial Pharmacy Research Lab, Shri G. S. Institute of Technology and Science, Indore, Madhya Pradesh 452003, India

Biopolymeric nanocarriers have become potential candidates for drug delivery applications due to outstanding virtues such as biodegradability, biocompatibility, low toxicity and low cost. The present study involves the synthesis of such biopolymeric nanocarriers prepared from Aloe vera gel, conjugated with antihypertensive model drugs (atenolol, bisoprolol and propranolol) using ionotropic gelation-polyelectrolyte complexation and the determination of entrapment efficiencies, *in vitro* release of these drugs from nanoparticles followed by the study of release kinetics. The synthesized antihypertensive drug-loaded nanoparticles were undertaken for characterization using Ultraviolet-Visible spectroscopy, Scanning Electron Microscopy, Fourier Transform Infra-red Spectroscopy and Zeta potential measurements and Powder X-ray diffraction analysis. The analysis ended up with confirmation of the semi-crystalline nature of the synthesized drug-loaded nanoparticles with an average size of 86.97±2.17 nm, 78.32±1.97 nm and 89.36±2.15 nm for atenolol, bisoprolol and propranolol loaded Aloe vera (gel) nanoparticles respectively determined with X-ray diffraction analysis. Atenolol and Bisoprolol loaded Aloe vera gel nanoparticles using barium chloride and Propranolol loaded Aloe vera gel nanoparticles using barium chloride followed Korsmeyer-Peppa's model for drug release with Anomalous (non-Fickian) transport.

Key words: Ionotropic gelation, nanoparticles, Aloe vera gel, antihypertensive drugs, biopolymeric nanoparticles

Over the years, there has been an increasing interest in designing biopolymer-based drug delivery systems to achieve the therapeutic effect at controlled rates[1-4]. Mostly, for controlled delivery of drugs the oral route is preferred because of its convenience and ease of administration along with greater flexibility in dosage form design, production and cost-effectiveness.

Aloe vera (*Aloe barbadensis* Miller) is a perennial succulent xerophyte belonging to the family Liliaceae. Aloe vera gel has been reported to have more than 75 potentially active ingredients[5,6]. Aloe vera gel is receiving much scientific attention due to its diverse composition[5] and enormous properties such as antifungal[7], antioxidant[8], burn and wound healing[9,10], antibacterial[11], antiseptic[12], antiviral[13-15], anti-inflammatory, hepatoprotective and many more[16].

Apart from these applications the properties of Aloe vera gel have also been explored for the synthesis of nanoparticles (mainly with metals such as silver and gold for studying their antimicrobial activities), microparticles (in combination with Chitosan and Vitamin E for skin burn treatment)[17], films (in combination with alginate contributed to mechanical and thermal property enhancement)[9], nanoemulsions

***Address for correspondence**
E-mail: sharmarachana385@gmail.com

Accepted 10 May 2023
Revised 30 June 2023
Received 02 December 2021
Indian J Pharm Sci 2023;85(3):632-643

(with alginate to increase oral delivery of insulin)[18] and enhancement of bioavailability of vitamin C and E[19], as drug carrier (in the formulation of hydrogel with ascorbic acid)[20].

Beta-blockers are a group of drugs that hinder the sympathetic activation of β-adrenergic receptors. Cardioselective blockers (e.g., Atenolol (ATE), Bisoprolol (BIS)) primarily block β1 receptors on the heart, thereby reducing heart rate, cardiac contractility, cardiac workload, etc. On the other hand, non-selective beta-blockers (e.g., Propranolol (PRO)) inhibit β1 receptors and may cause bronchoconstriction, peripheral vasoconstriction, and metabolic imbalances (e.g., hypoglycemia and hyperglycemia) in addition to cardiac effects[21]. Hence, there is a need of developing such a system that can deliver drugs without causing any side effects, and thus an attempt was made to design a biopolymeric nanocarrier system that can overcome these problems. ATE, PRO along with BIS (considered to be a potent drug with a longer half-life) were used as model drugs[22].

Ionotropic gelation is a well-known method[23] to obtain nanoparticles due to its ease, non-toxicity, and cost-effectiveness. Several studies involving ionotropic gelation have been reported and polymers like chitosan, poly-l-lysine, and Polyethyleneimine (PEI) have been considerably used for this purpose[24-29]. The poly-D-galacturonate sequences of pectin can form a gel in presence of divalent ions such as Ca^{2+} or Ba^{2+} and undergo egg-box structure[30]. Hence we have used barium chloride as a cross-linker. This study aimed to prepare antihypertensive drugs loaded nanoparticles from Aloe vera gel (in dry powdered form) using Ionotropic gelation with the determination of drug entrapment followed by the study of *in vitro* drug release.

MATERIALS AND METHODS

Materials:

Aloe vera gel powder was procured from Aatur Instruchem (Vadodara) and was compared with fresh Aloe vera gel extracted from the Aloe vera plant. ATE, BIS and PRO drugs were obtained as gift samples; PEI was purchased from Loba Chemie, Mumbai. BaCl2 was purchased from Merck. Other chemicals used were pharmaceutical and analytical grades.

Methods:

Preparation of blank polysaccharide-based nanoparticles: Blank Aloe vera Gel Nanoparticles (AGBC NPs) were prepared by Ionotropic gelation followed by polyelectrolyte complexation, reported by Rajaonarivony *et al.*[23], with certain modifications as mentioned below. The preparation of nanoparticles is a two-step process.

Step I: 2 ml Barium Chloride (BC) (3.35 mg/ml, w/v) was added dropwise to 10 ml Aloe vera gel aqueous solution (3 mg/ml, w/v) to induce gellification while stirring for 30 min using a magnetic stirrer (Remi, India) at 1200 rpm.

Step II: 4 ml PEI solution [0.8 mg/ml, (w/v)] was added drop-wise into the above obtained pre-gel solution to form a polyelectrolyte complex and was stirred for an hour at 1200 rpm. The resultant suspension was kept overnight. The nanoparticles thus formed were separated by using a cooling centrifuge at 18 000 rpm for 45 min and dried under lyophilizer at -78° for 24 h using D-Mannitol (5 % solution in distilled water) as a cryoprotectant.

Preparation of drug loaded Aloe vera gel nanoparticles: 2 ml aqueous solution (optimum concentration 500 ppm) of drugs ATE/BIS/PRO drug was incorporated into 10 ml Aloe vera gel aqueous solution (3 mg/ml, w/v) and rest of the process was same as described for the preparation of blank nanoparticles (fig. 1).

Physicochemical characterization:

Fourier Transform Infrared (FT-IR) spectra were recorded by using KBr pellets on FT-IR Jasco FT-IR-4600. Zeta potential was determined by using Malvern Zeta Sizer Nano ZS and Nano Plus. Powder X-Ray Diffraction (PXRD) measurements were performed using Bruker D8 advanced X-Ray diffractometer using CuKα radiation (λ=0.154 nm). The size of the nanoparticles was calculated by Debye-Scherrer equation ($D=0.9\lambda/\beta \cos \theta$), where D is the crystal size, λ is the wavelength of X-ray, θ is the Bragg's angle in radians, and β is the Full Width at Half Maximum (FWHM) of the peak in radians[31]. The area of the peaks at 2θ values had been considered as the representative peaks for calculation of crystallinity index i.e. percentage crystallinity calculated by using the following equation

$$\% \text{ crystallinity} = Ic/(Ic+Ia)\times 100 \text{---------}(1)$$

Where, Ia and Ic are the integrated intensities corresponding to the amorphous and crystalline phases, respectively[32]. The morphology of synthesized blank and drug-loaded nanoparticles was examined by Scanning Electron Microscopy (SEM) (SEM-JEOL-JSM-5600 and EVO 18, Carl Zeiss, UK) instruments operated at 20 kV and 6.0 kV respectively.

Determination of drug content and entrapment efficiency: The assay of individual drugs (70±3 %) was performed and the amount of drugs (ATE, BIS and PRO) loaded on Aloe vera gel nanoparticles was determined by UV-Visible spectrometer (Perkin Elmer, Lambda 75). The drug-loaded nanoparticles suspension was centrifuged at 18 000 rpm for 30 min (at 4°) using a cooling centrifuge (Thermo). The supernatant solution was separated and the amount of free drug in the supernatant solution was determined by UV-Visible spectrometer at 224 nm, 223 nm and 288 nm for ATE, BIS and PRO respectively in distilled water. Drug content was calculated using the calibration curve and percentage AE[33] was calculated using the following formula

% AE=Total drug-Free drug/Total drug×100----(2)

***In vitro* release studies of the drugs:** The *in vitro* release studies of ATE, BIS and PRO-loaded Aloe vera gel nanoparticles were carried out by using a dialysis membrane. The drug-loaded nanoparticles (equivalent to 25 mg of drug) were dissolved in 10 ml distilled water and taken in a dialysis bag (molecular weight cut off 20 kDa, pore size 0.2 µm), and were placed in a beaker containing 100 ml distilled water. The medium was agitated continuously at 50 rpm using a magnetic stirrer and the temperature was maintained at 37±0.5°. 5 ml sample was withdrawn at various time intervals throughout 48 h and fresh distilled water was replaced during each sampling. The amount of drug released was determined by UV-Visible spectrometer at respective λ_{max} values of drugs[34].

***In vitro* drug release kinetics:** The drug release data were fitted into different kinetics models such as Zero order, First order, Higuchi Model, Hixon-Crowell's cube root equation, and Korsmeyer-Peppa's Power-Law Equation Model to understand the kinetics and drug release mechanism from nanoparticles. The methods were adopted to investigate the most suitable model[35,36].

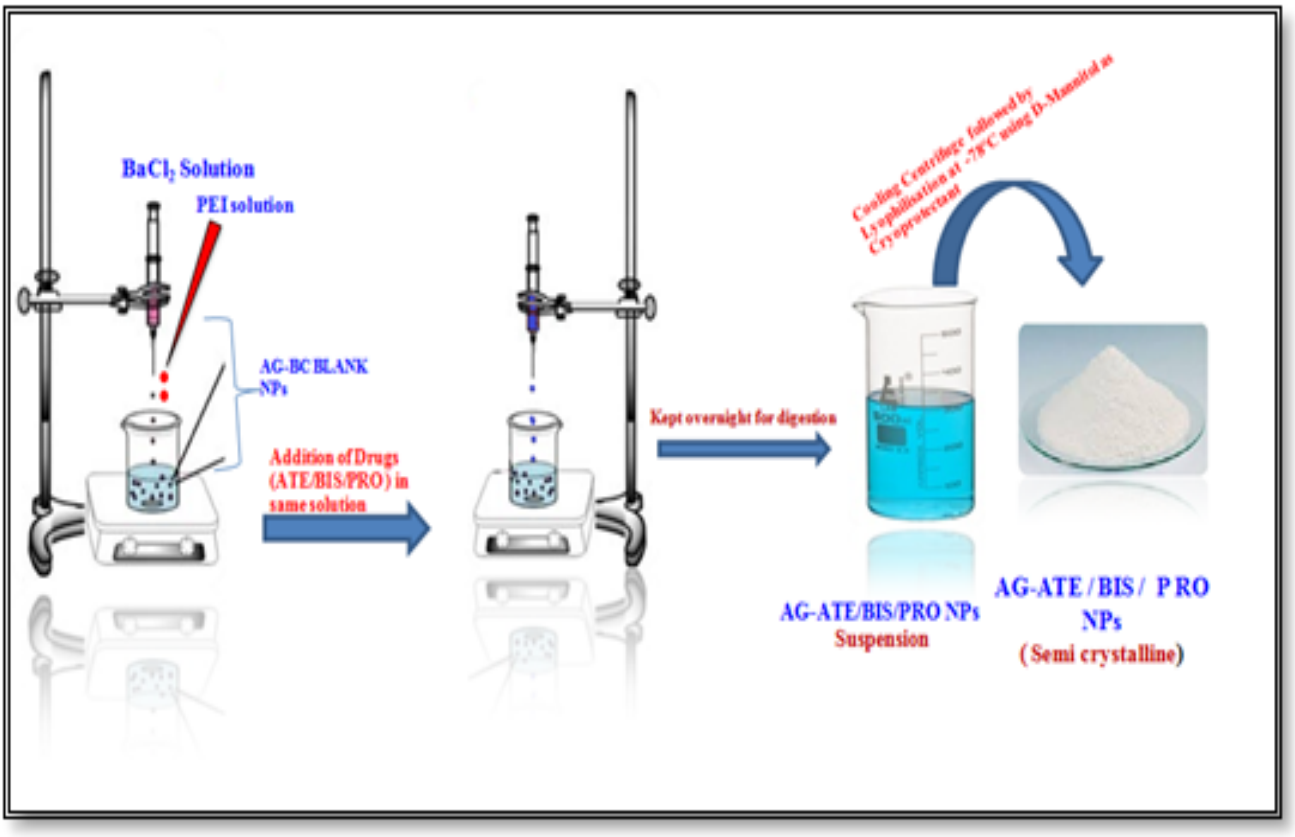

Fig. 1: Experimental set-up for preparation of nanoparticles

RESULTS AND DISCUSSION

Aloe vera gel nanoparticles were prepared by ionotropic gelation coupled with polyelectrolyte complexation where PEI, a polycationic polymer and pectin (polygalacturonate sequences) present in Aloe vera gel, a polyanionic polymer are combined through a cross-linker Ba^{2+}. Pectin present in Aloe vera exhibits an excellent property of gelling in the presence of divalent cations[37]. The mechanism of gelation involves the formation of egg-box structures[30,38,39] with divalent Ba^{2+} cations and hydrogen bonding with water. The mixing of two oppositely charged polyelectrolyte solutions results in a turbid solution confirming the formation of polyelectrolytes. PEI seems to act together with pectin to form a polyelectrolyte complex and probably contributes to gel porosity and acts as a physical barrier to drug release[40]. Hence it can be assumed that ionotropic gelation initially results in the formation of AG-BC complexes which involves the interactions between Ba^{2+} and polygalacturonic sequences of pectin (Aloe vera gel), an aid for the formation of egg-box structure, leading to the formation of gel which entraps drugs within it and gradually releases the drug (fig. 2).

The successful attempt for the synthesis of Aloe vera gel NPs was initially evaluated by using FT-IR. In the FT-IR spectrum of Aloe vera gel (fig. 3a-fig. 3c) broad absorption band observed at 3423 cm^{-1} is due to the stretching of –OH groups, a characteristic of carbohydrate monomers[41-44]. The absorption band at 2923.6 cm^{-1} can be due to the symmetrical and asymmetrical C-H stretching of aliphatic –CH and $–CH_2$ groups. The absorption peak present at 1740 cm^{-1} characteristic of C=O stretching indicates the presence of carbonyl groups in Aloe vera gel. The absorption peaks at 1647.88 cm^{-1} and 1410.67 cm^{-1} respectively are associated with the asymmetrical and symmetrical COO– stretching of carboxylate group of pectin present in Aloe vera gel. The absorption band at 1257.36 cm^{-1} is attributed to the C-O-C stretching of the $–COCH_3$ group and the absorption band at 1072.23 cm^{-1} may correspond to C-O stretching associated with rhamnogalacturonan, pectin present in Aloe vera gel. An absorption peak at 870 cm^{-1} is due to the C-H out-of-plane deformation of carbohydrate monomers[44].

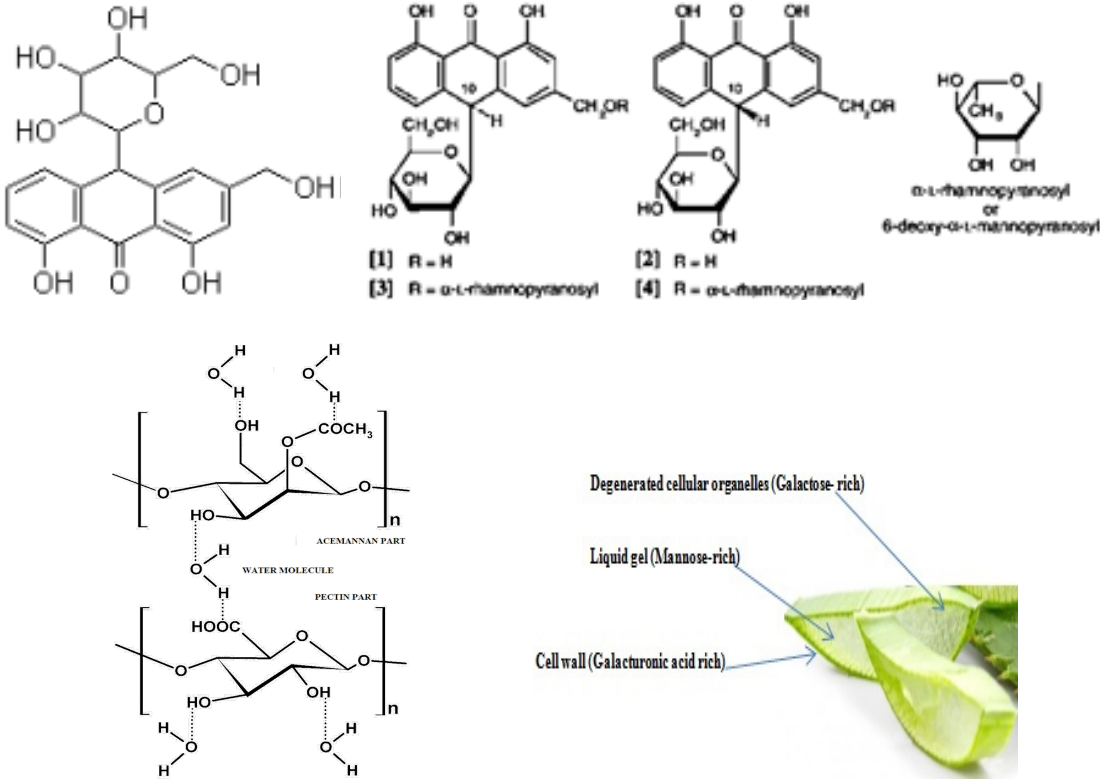

Fig. 2: Chemical structure of (a) Phenolic compound (Aloin); (b) Some polysaccharide constituents of Aloe vera gel[41]; (c) Illustration of H-bond formation (shown by dotted line) between water molecule and acemannan or pectin present in Aloe vera gel and (d): Cross-sectional area of Aloe vera gel

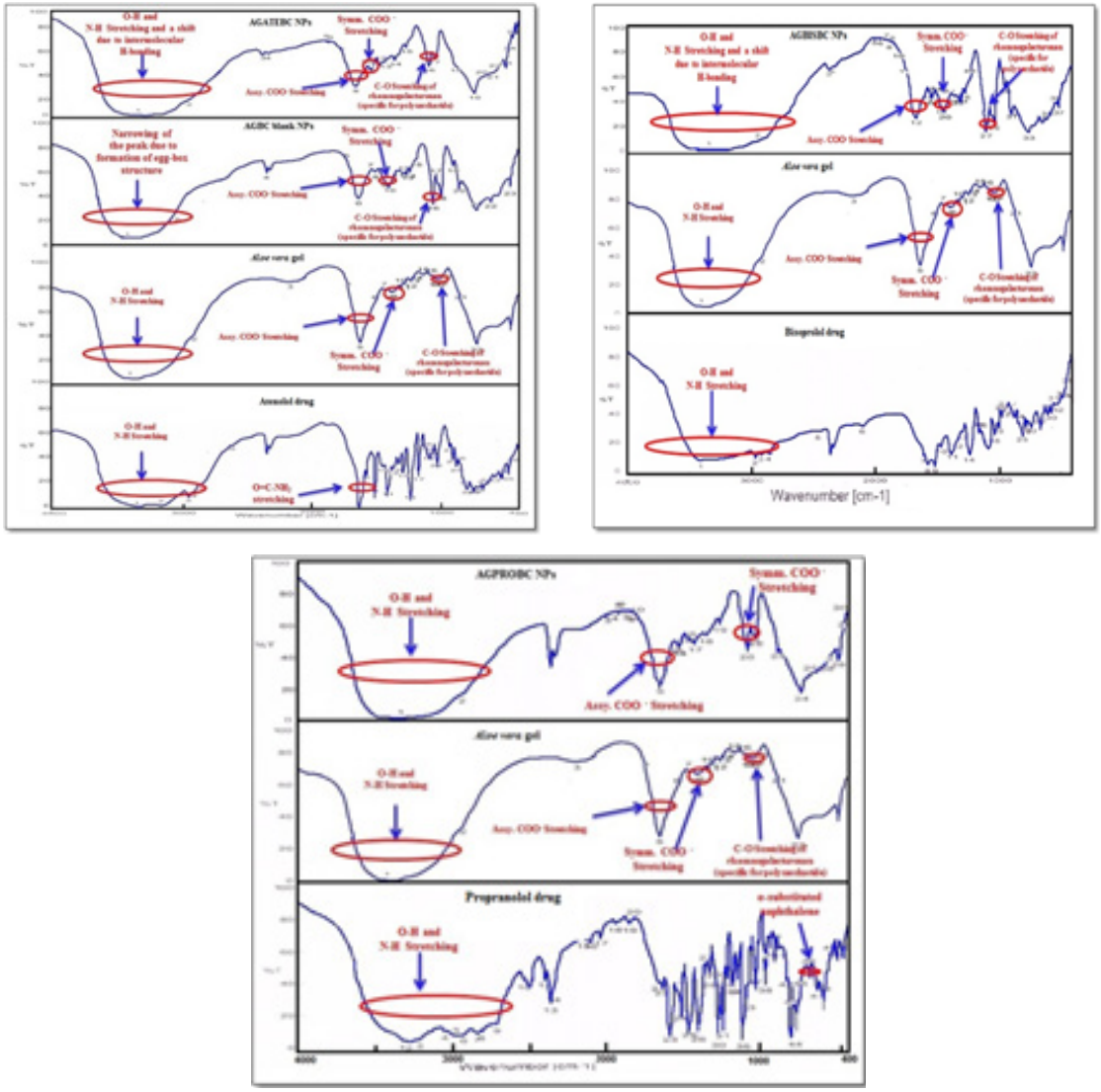

Fig. 3: FT-IR spectra of (a): Atenolol drug, Aloe vera gel, AGBC blank NPs and AGATEBC NPs; (b): Bisoprolol drug, Aloe vera gel and AGBISBC NPs and (c): Propranolol drug, Aloe vera gel and AGPROBC NPs

The bands observed in the spectrum after crosslinking with Ba^{2+} ions are very significant. Absorption regions of stretching vibrations of O-H bonds in blank AGBC NPs appear narrow than that obtained in native Aloe vera gel. This difference arises from the participation of hydroxyl group and carboxylate groups of Pectin present in Aloe vera gel to the barium ion to form a chelating structure and consequent decrease in Hydrogen-bonding which results in narrowing of the band in AGBC NPs (fig. 3a).

The FT-IR spectrum of ATE drug (fig. 3a) shows peaks ate 3362.28 cm^{-1} for O-H stretching, at 3174.26 cm^{-1} for N-H stretching, at 2965.02 cm^{-1} for C-CH3 stretching, at 1581 cm^{-1} for C=C aromatic stretching, at 1732.1 cm^{-1} for C=O stretching and 1637.22 cm^{-1} for O=C-NH2 stretching[34]. The interaction between polymer and drug can be identified by the shifting or disappearance of the frequency of functional characteristic peaks. FT-IR spectrum of AGATEBC NPs (fig. 3a) shows characteristic peaks of both polymer and drug. As evident from the FT-IR spectrum of AGATEBC NPs, a shift in peak responsible for O-H stretching (3423 cm^{-1}) of Aloe vera gel to a lower frequency (3320.82 cm-1) is observed

The FT-IR spectrum of BIS drug (fig. 3b) shows principal absorption peaks at 3347.5 cm^{-1}, 3407.6 cm^{-1} attributed to N-H stretching and O-H stretching respectively at 1613.36 cm^{-1} and 1577.49 cm^{-1} for C-O stretching, 1514.81 cm^{-1} for C-C aromatic stretching, 1097.3 cm^{-1} for C-O-C stretching and 1145.51 cm^{-1} for C-O stretching vibrations[45]. The FT-IR spectrum of AGBISBC NPs (fig. 3b) shows characteristic peaks of both

polymer and drug. FT-IR spectrum of AGBISBC NPs shows a shift in peak corresponding to O-H stretching (3423 cm^{-1}) to a lower frequency of 3327.57 cm-1.

The FT-IR spectrum of PRO drug in fig. 3c shows a characteristic peak at 3282.25 cm^{-1} which corresponds to O-H stretching of the secondary Hydroxyl group, at 2926.45 cm^{-1} for N-H stretching, at 1267.97 cm^{-1} for aryl-O-CH2 (C-O-C) asymmetric stretching, an aryl -O-CH2 (C-O-C) symmetric stretching at 1041.37 cm^{-1} and a peak at 790.67 cm^{-1} attributed to the presence of α-substituted naphthalene[46].

The FT-IR spectrum of AGPROBC NPs, fig. 3c shows characteristic peaks of both polymer and drug. There is a small shift in peak responsible for O-H stretching (3423 cm^{-1}) to a lower frequency (3340 cm^{-1}) is observed. The difference in the FT-IR spectra of AGBC NPs and the drug-loaded Aloe vera gel nanoparticles (AGATEBC, AGBISBC, and AGPROBC NPs) shows decrease in the sharpness of the peaks and shifts in the characteristic frequencies of respective functional groups. The shifts in frequencies corresponding to O-H stretching, towards the lower side may be attributed to electrostatic interaction/Hydrogen bonding between amine groups of drug and –OH groups of pectin present in Aloe vera gel. Similarly, a small shift in asymmetric and symmetric stretching of the carboxylate functional group is observed which indicates successful loading of drugs (ATE, BIS, and PRO) on Aloe vera gel nanoparticles and incorporation of the drug in the gel system is through intermolecular hydrogen-bonding between the electropositive amino hydrogen of a drug molecule and the electronegative carboxylate ions of pectin found in Aloe vera gel.

The zeta potential value provides information about the colloidal stability of the prepared nanoparticles suspension and is highly affected by the particle's surface charge. Particles with large positive or negative zeta potentials form stable colloidal suspension where the particles tend to repel each other thereby reducing particle aggregation. The zeta potential of blank Aloe vera gel nanoparticles is found to be –29.3±1.3 mV. The negative zeta potential is due to the presence of residual carboxylate end groups present on the surface of pectin found in Aloe vera gel[47]. As denoted by results in Table 1, AGATEBC NPs, AGBISBC NPs and AGPROBC NPS show the negative value of zeta potential out of which AGBISBC NPs (-45.11±2.30 mV) indicates the most stable nature and the negative surface charge is due to the presence of residual carboxylate and hydroxyl ions on the surface of pectin (Aloe vera gel).

The PXRD patterns of AGATEBC NPs, AGBISBC NPs, and AGPROBC NPs are shown in fig. 4a-fig. 4c. The amorphous nature of the Aloe vera gel nanocarrier has been confirmed by the XRD patterns appearing as a broad peak. However, the diffractograms of AGBC NPs show some sharp peaks which reveal that barium ions increase the crystallinity of the Aloe vera (gel) chains because the polysaccharide, pectin (Poly-D-galacturonate sequences) present in Aloe vera gel undergo formation of egg-box[38,48] or cage box structure in presence of divalent ions (Ca^{2+} or Ba^{2+} ions)[37] as shown in fig. 5.

TABLE 1: STRUCTURAL CHARACTERISTICS, ENTRAPMENT EFFICIENCY OF AGATEBC NPs, AGBISBC NPs, AND AGPROBC NPs

S. No	Sample Name (NPs)	Drugs (Half-life)	ZP (mV)	Crystallinity Index or % Crystallinity of drugs (%)		Particle size by XRD (nm)	Entrapment Efficiency (AE) (%)
				Before loading on AG NPs	After loading on AG NPs		
1	AGATEBC NPs	Atenolol (6-7 h)	-33.94±1.74	63.03	20.16	86.97±2.17	55.15±1.19
2	AGBISBC NPs	Bisoprolol (10-12 h)	-45.11±2.30	58.9	38.67	78.32±1.97	73.05±1.57
3	AGPROBC NPs	Propranolol (3-5 h)	-26.30±1.17	64.94	29.45	89.36±2.15	89.43±1.48

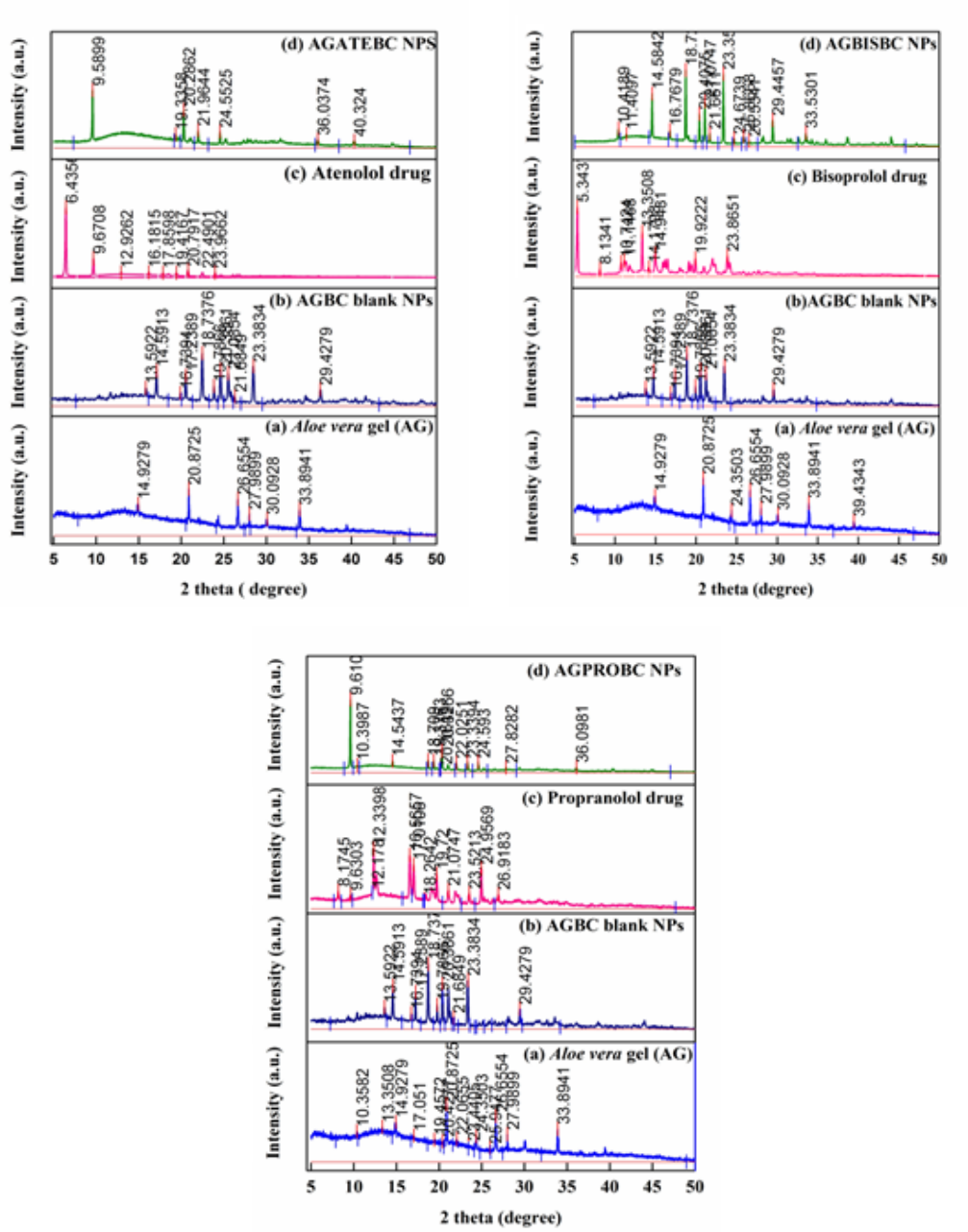

Fig. 4: XRD patterns of (a): AGATEBC NPs; (b): AGBISBC NPs and (c): AGPROBC NPs

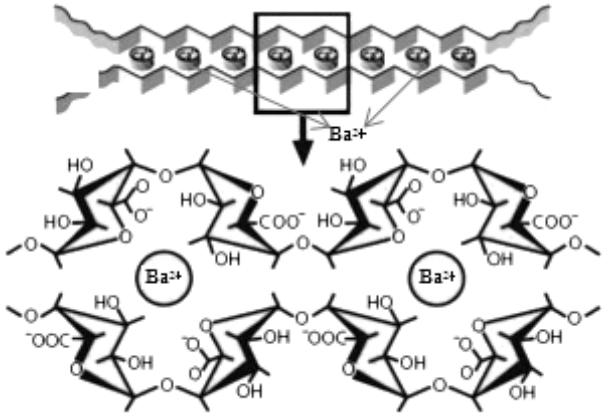

Fig. 5: Schematic representation of barium binding to polygalacturonate sequences of pectin (of Aloe vera gel) 'egg-box' dimers and 'egg-box' cavity[48]

The purpose of PXRD analysis was to determine whether the entrapped drugs existed in a crystalline or amorphous state. Pure drugs show diffractograms consistent with their crystalline nature since they exhibited several intense characteristic peaks. On the other hand, some of the sharp peaks observed in pure drugs were not visible in the diffraction patterns of drug-loaded nanoparticles suggesting that the drugs entrapped in Aloe vera gel nanoparticles existed in an amorphous state which also indicates that an XRD signal of entrapped or encapsulated drug is very difficult to detect[49,50]. Thus, the crystallographic data indicate that the % crystallinity of all three drugs decreased (Table 1) suggesting the change of drugs from their crystalline state to an amorphous state provided with increased solubility of the entrapped drug as compared to the crystalline state. This observation confirms the successful and homogeneous incorporation and entrapment of drugs in gel structure (Aloe vera gel) as compared to a crystalline state, although the crystallinity of Aloe vera gel is increased and thus we obtain semi-crystalline nanoparticles[37].

The decrease in crystallinity of drugs can also be correlated with the difference in the IR spectrum of pure drugs and drugs entrapped within the polymer matrix. The IR spectra of pure drugs contain several sharp peaks (with high intensity) in contrast; the IR spectra of drugs after entrapment within Aloe vera gel nanoparticles show broad peaks (with low intensity) along with some additional peaks[51,52].

The average particle size of blank nanoparticles and drug-loaded nanoparticles is shown in Table 1. The particle size of AGBISBC NPs is found to be relatively smaller which may be due to encapsulation of the drug within AGNPs. It is assumed that the larger size of AGATEBC NPs and AGPROBC NPs is attributed to the adsorption of ATE and PRO drugs onto the surface of AGNPs. SEM results show the porous nature of Aloe vera gel and fibrous (fig. 6a), rod-like morphology is exhibited by drug-loaded Aloe vera gel nanoparticles along with nanoparticle aggregation (particle size is denoted on micrometer scale due to aggregation and only the morphology is determined with SEM analysis). The presence of pores is closely related to the swelling behavior of Aloe vera gel and its ability to absorb water. Interstitial spaces of pores allow water to get absorbed on the surface followed by diffusion of water towards the center of the gel due to capillary force[49,53].

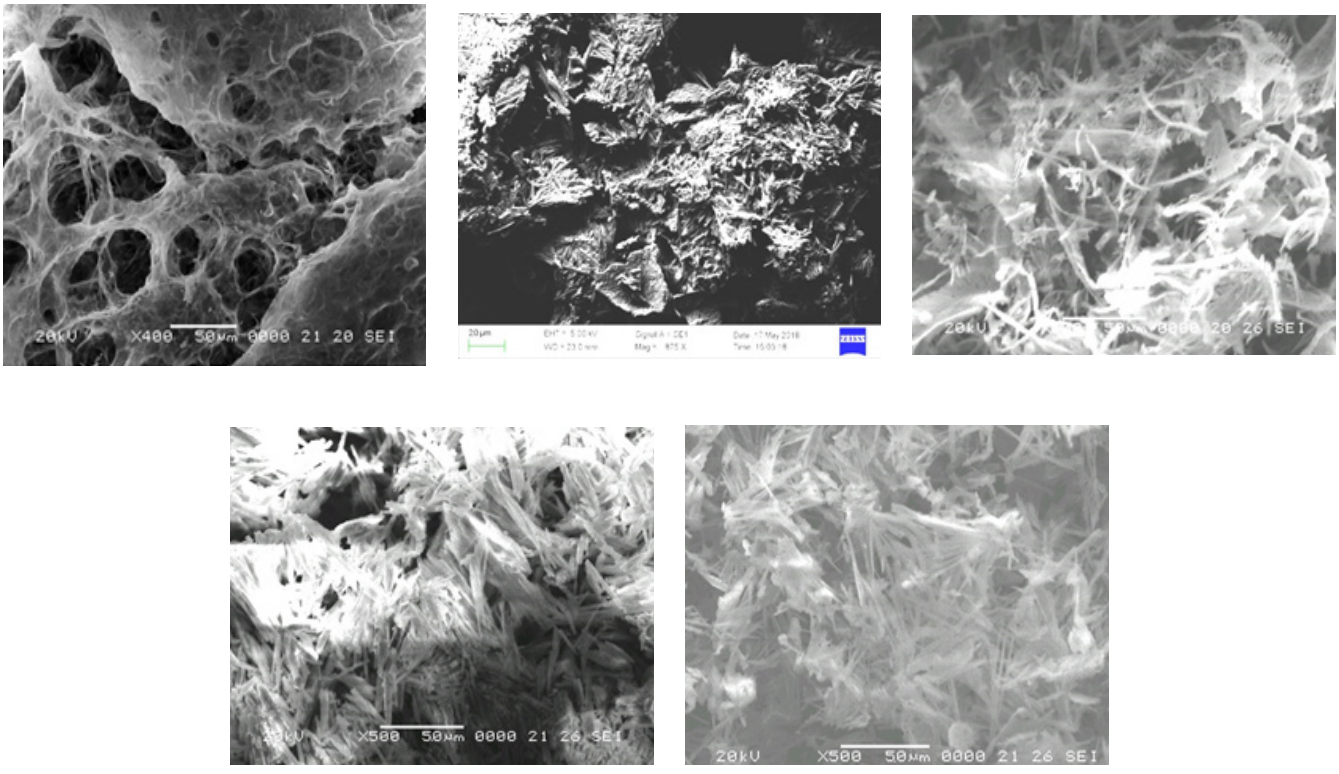

Fig. 6: SEM Micrographs of (a): Aloe vera gel; (b): AGBC NPs; (c): AGATEBC NPs; (d): AGBISBC NPs and (e): AGPROBC NP

As the drug is incorporated into the polymer matrix the free spaces get occupied by drug molecules resulting in more compact structures of drug-loaded Aloe vera gel nanoparticles[53]. The AGBC NPs (fig. 6b) exhibit solid rod-like morphology with smooth surfaces whereas AGATEBC NPs (fig. 6c) and AGBISBC NPs (fig. 6d) show fibrous morphology. In contrast, AGPROBC NPs (fig. 6e) show regular, rod-like, closely arranged structures (relatively more compact). The compactness in morphology increases on moving from AGATEBC NPs to AGBISBC NPs and is highest in the case of PRO-loaded Aloe vera gel nanoparticles suggesting the highest entrapment (89.43±1.48 %) of PRO drug by Aloe vera gel nanoparticles and therefore, the least release of drug from AGPROBC NPs is observed. It can be predicted from the results that the increase in compactness in PRO loaded Aloe vera gel nanoparticles involved pi-pi aromatic stacking due to the presence of naphthalene in the chemical structure of the PRO drug[54,55]. The decrease in porosity and increase in regularity in the morphology of the polymer matrix itself indicate successful entrapment of the drugs by Aloe vera gel nanoparticles.

Moreover, the differences in SEM images before drug loading (blank nanoparticles) and after drug loading due to aggregation of nanoparticles is indicative of successful loading of drugs, thus no size calculations were made with these data due to aggregation of nanoparticles hence results obtained by XRD analysis have been considered to be ultimate for size. (Although the DLS analysis was also performed but due to the aggregation of nanoparticles the size results were found in micrometer range hence were not considered).

The amount of drug in nanoparticles was calculated using a calibration curve at λ_{max} values 224, 223 and 288 nm for ATE, BIS, and PRO drugs respectively in distilled water (pH 6.8-7.0). The entrapment efficiency of Aloe vera gel nanoparticles was greatly influenced by drug concentrations hence different concentrations of drugs were loaded on NPs and then an optimized concentration (500 ppm or 500 µl) of the drug was used to prepare nanoparticles. The entrapment efficiency of drug-loaded Aloe vera gel nanoparticles was found in the range of 55.15±1.19 % to 89.43±1.48 % (Table 1). The highest entrapment efficiency is shown by PRO-loaded Aloe vera gel nanoparticles and it is in agreement with the results obtained by SEM analysis where a highly compact structure is exhibited by AGPROBC NPs.

The *in vitro* release behavior of ATE, BIS and PRO drugs from AGATEBC NPs, AGBISBC NPs, and AGPROBC NPs respectively were investigated and the comparative results are shown in fig. 7a (bar charts for mean with standard error are provided in supplementary material) and in Table 1.

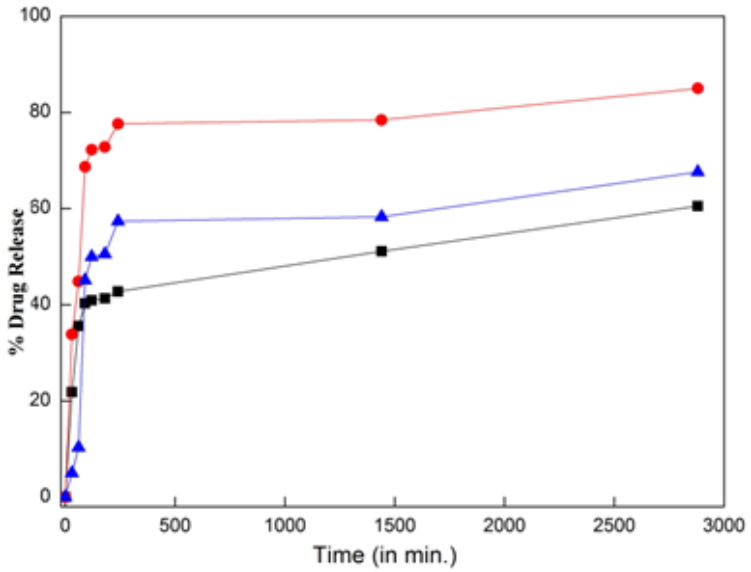

Fig. 7: *In vitro* release profiles of Atenolol, Bisoprolol and Propranolol drugs from AGATEBC NPs, AGBISBC NPs and AGPROBC NPs respectively
Note: (▪): AGPROBC 500; (●): AGBISC 500 and (▲): AGATEBC 500

In the case of ATE-loaded Aloe vera gel nanoparticles an initial burst release of say about 21-35 % is observed in the first 30-60 min, which might be associated with the porous and hydrophilic nature of Aloe vera gel. Afterward, the release medium penetrated the drug-loaded nanoparticles and dissolved the entrapped ATE drug. These results show that the key factors which affect the drug release from AGATEBC NPs exhibited sustained release from the nanoparticles and a cumulative release ratio reached approximately 58 % over 24 h followed by switching of drug release pattern to a very slow release phase[29,56] where around 67 % of entrapped ATE drug was released for 48 h.

AGBISBC NPs and AGPROBC NPs followed the same patterns of drug release but the release amounts are different. The total amount of the drug released from AGBISBC NPs is around 84.98 %. In contrast; the total amount of drug released from AGPROBC NPs is about 60.53 % which is consistent with the results under SEM analysis where a highly closed or dense morphology is exhibited by AGPROBC NPs with the highest entrapment efficiency (~89 %) and thus relatively low drug release ~60 %. These results suggest that the release of ATE, BIS and PRO drugs from Aloe vera gel nanoparticles was retarded significantly due to the entrapment of these drugs within the Aloe vera gel nanoparticles and hence this nanoparticulate formulation can be used for slow drug release[57].

Based on the best fit with the highest correlation (R^2) value, it is concluded that AGATEBC NPs, AGBISBC NPs and AGPROBC NPs follow the Korsmeyer-Peppa's Power-law equation model[58] with Anomalous non-Fickian diffusion i.e. the rate of solvent penetration and drug release are in the same manner indicating increased drug diffusivity from the matrix by solvent-induced relaxation of the polymer Aloe vera gel. Korsmeyer-Peppa's model involves a plot of log (cumulative % drug released) *vs.* log (time) that yields a slope 'n' diffusion exponent. If n=0.5, it indicates Pure-Fickian diffusion, if n=0.5-1 or n=0.45-0.89, indicates Anomalous non-Fickian diffusion[59].

Generally, swellable polymeric devices (like Aloe vera in the current case) follow Korsmeyer-Peppa's model and the use of this power-law equation for analyzing drug release data from a porous system often lead to n<0.5, indicating combined mechanism (diffusion through the matrix and partially from water-filled pores causing a shift in the release exponent (n) towards smaller values as is the case with AGPROBC NPs (where n=0.48) representing porous systems (following SEM results where porous morphology is shown by starting material –Aloe vera gel). Thus from the results, it can be concluded that the drug release from PRO-loaded Aloe vera gel NPs was through the combination of bulk degradation along with diffusion[36]. The kinetic plots for Korsemeyer- Peppa's model for all systems and the results are summarized in Table 2.

TABLE 2: DIFFERENT MODELS IN TERMS OF R^2 AND RELEASE EXPONENT (n)

Model name	AGATEBC NPs		AGBISBC NPs		AGPROBC NPs	
	R^2	Slope(n)	R^2	Slope(n)	R^2	Slope(n)
Zero order	0.35	0.016	0.25	0.001	0.43	0.011
First order	0.46	0	0.5	0	0.59	0
Higuchi's model	0.53	1.081	0.43	0.68	0.62	0.79
Hixon -Crowell Cube -Root equation Model	0.42	0	0.44	1.064	0.75	0
Korsmeyer-Peppa's Power Law Equation Model	0.8	0.571	0.74	0.53	0.77	0.482

The present study explored the possibility of preparing antihypertensive drug-loaded Aloe vera gel nanoparticles without using any organic solvent. The FT-IR, SEM, and XRD results indicated that drugs have been successfully incorporated into Aloe vera gel resulting in semi-crystalline nature. Aloe vera gel nanoparticles loaded with antihypertensive drugs have demonstrated greater entrapment efficiencies ranging from 55.15±1.19 % to 89.43±1.48 %. The 'n' value indicated that the release mechanism follows Anomalous (non-Fickian) transport. These results point that Aloe vera gel nanoparticles can be effectively utilized for pharmaceutical and biomedical applications especially in the field of bio encapsulation and delivery of hydrophilic or fragile drugs.

Acknowledgments:

Authors highly acknowledge Dr. Shubha Jain, Professor and Head, School of Studies in Chemistry and Biochemistry, Vikram University, Ujjain (M.P.) for her endless guidance and support, Parul Group of Institutes, Vadodara (Gujarat) for providing analysis facility(zeta potential and DLS). Dr. G.S. Okram and Dr. Mukul Gupta, Dr. L. Bahera, (XRD), Dr. D.M. Phase, Mr. Vinay Ahire (SEM), UGC-DAE CSR, Indore (M.P.), for providing lab facilities and Central University, Gandhinagar (Gujarat) for SEM analysis.

Conflict of interests:

The authors declared no conflict of interests.

REFERENCES

1. Chen W, Lu Z, Viljoen A, Hamman J. Intestinal drug transport enhancement by Aloe vera. Planta Med 2009;75(06):587-95.
2. Pramanik A, Sahoo RN, Nanda A, Mohapatra R, Singh R, Mallick S. Ocular permeation and sustained anti-inflammatory activity of dexamethasone from kaolin nanodispersion hydrogel system. Curr Eye Res 2018;43(6):828-38.
3. Panda B, Subhadarsini R, Mallick S. Biointerfacial phenomena of amlodipine buccomucosal tablets of HPMC matrix system containing polyacrylate polymer/β-cyclodextrin: Correlation of swelling and drug delivery performance. Expert Opin Drug Deliv 2016;13(5):633-43.
4. Satapathy SR, Sahoo RN, Satapathy B, Immani R, Panigrahi L, Mallick S. Development and characterization of leuprolide acetate encapsulated PLGA microspheres for parenteral controlled release depot injection. Indian J Pharm Edu Res 2021;55(1):107-16.
5. Sharma R. An overview of future prospect of Aloe vera gel as nano drug carrier. Technologies for sustainable rural development having potential of socioeconomic upliftment. (Shukla, JP ed.) Allied Publishers, New Delhi. 2014:173-9.
6. Tippayawat P, Phromviyo N, Boueroy P, Chompoosor A. Green synthesis of silver nanoparticles in aloe vera plant extract prepared by a hydrothermal method and their synergistic antibacterial activity. PeerJ 2016;4:e2589.
7. de Rodrıguez DJ, Hernández-Castillo D, Rodrıguez-Garcıa R, Angulo-Sánchez JL. Antifungal activity *in vitro* of Aloe vera pulp and liquid fraction against plant pathogenic fungi. Ind Crop Product 2005;21(1):81-7.
8. Hu Y, Xu J, Hu Q. Evaluation of antioxidant potential of Aloe vera (*Aloe barbadensis* Miller) extracts. J Agri Food Chem 2003;51(26):7788-91.
9. Pereira R, Tojeira A, Vaz DC, Mendes A, Bártolo P. Preparation and characterization of films based on alginate and aloe vera. Int J Polym Anal Charact 2011;16(7):449-64.
10. Davis RH, Donato JJ, Hartman GM, Haas RC. Anti-inflammatory and wound healing activity of a growth substance in Aloe vera. J Am Podiatr Med Assoc 1994;84(2):77-81.
11. Banu A, Sathyanarayana BC, Chattannavar G. Efficacy of fresh Aloe vera gel against multi-drug resistant bacteria in infected leg ulcers. Australas Med J 2012;5(6):305-9.
12. Surjushe A, Vasani R, Saple DG. Aloe vera: A short review. Indian J Dermatol 2008;53(4):163.
13. Athiban PP, Borthakur BJ, Ganesan S, Swathika B. Evaluation of antimicrobial efficacy of Aloe vera and its effectiveness in decontaminating gutta percha cones. J Conserv Dent 2012;15(3):246.
14. Ho MH, Hsieh CC, Hsiao SW, Thien DV. Fabrication of asymmetric chitosan GTR membranes for the treatment of periodontal disease. Carbohydr Polym 2010;79(4):955-63.
15. Feily A, Namazi MR. Aloe vera in dermatology: A brief review. G Ital Dermatol Venereol 2009;144(1):85-91.
16. Liu C, Cui Y, Pi F, Cheng Y, Guo Y, Qian H. Extraction, purification, structural characteristics, biological activities and pharmacological applications of acemannan, a polysaccharide from aloe vera: A review. Molecules 2019;24(8):1554.
17. Pereira GG, Santos-Oliveira R, Albernaz MS, Canema D, Weismüller G, Barros EB, *et al.* Microparticles of Aloe vera/ vitamin E/chitosan: Microscopic, a nuclear imaging and an *in vivo* test analysis for burn treatment. Eur J Pharm Biopharm 2014;86(2):292-300.
18. Basha SK, Muzammil MS, Dhandayuthabani R, Kumari *VS.* Development of nanoemulsion of Alginate/Aloe vera for oral delivery of insulin. Mater Today Proc 2021;36:357-63.
19. Vinson JA, Al Kharrat H, Andreoli L. Effect of Aloe vera preparations on the human bioavailability of vitamins C and E. Phytomedicine 2005;12(10):760-5.
20. Subramanian K, Narmadha S, Vishnupriya U, Vijayakumar V. Release characteristics of Aspirin and Paracetamol drugs from tablets with Aloe Vera gel powder as a drug carrier. Drug Invent Today 2010;2(9):424-8.
21. Frishman WH. Clinical significance of beta1-selectivity and intrinsic sympathomimetic activity in a beta-adrenergic blocking drug. Am J Cardiol 1987;59(13):F33-7.
22. McDevitt DG. Comparison of pharmacokinetic properties of beta-adrenoceptor blocking drugs. Eur Heart J 1987;8(suppl_M):9-14.
23. Rajaonarivony M, Vauthier C, Couarraze G, Puisieux F, Couvreur P. Development of a new drug carrier made from alginate. J Pharm Sci 1993;82(9):912-7.
24. Sarmento B, Martins S, Ribeiro A, Veiga F, Neufeld R, Ferreira D. Development and comparison of different nanoparticulate polyelectrolyte complexes as insulin carriers. Int J Peptide Res Ther 2006;12:131-8.
25. Woitiski CB, Sarmento B, Carvalho RA, Neufeld RJ, Veiga

F. Facilitated nanoscale delivery of insulin across intestinal membrane models. Int J Pharm 2011;412(1-2):123-31. [Crossref] [Google Scholar]]
26. Goycoolea FM, Lollo G, Remunán-López C, Quaglia F, Alonso MJ. Chitosan-alginate blended nanoparticles as carriers for the transmucosal delivery of macromolecules. Biomacromolecules 2009;10(7):1736-43.
27. Motwani SK, Chopra S, Talegaonkar S, Kohli K, Ahmad FJ, Khar RK. Chitosan–sodium alginate nanoparticles as submicroscopic reservoirs for ocular delivery: Formulation, optimisation and *in vitro* characterisation. Eur J Pharm Biopharm 2008;68(3):513-25.
28. Nagarwal RC, Kumar R, Pandit JK. Chitosan coated sodium alginate–chitosan nanoparticles loaded with 5-FU for ocular delivery: *In vitro* characterization and *in vivo* study in rabbit eye. Eur J Pharm Sci 2012;47(4):678-85.
29. Lopes M, Abrahim B, Veiga F, Seiça R, Cabral LM, Arnaud P, *et al.* Preparation methods and applications behind alginate-based particles. Expert Opin Drug Deliv 2017;14(6):769-82.
30. Powell DA, Morris ER, Gidley MJ, Rees DA. Conformations and interactions of pectins: II. Influence of residue sequence on chain association in calcium pectate gels. J Mol Biol 1982;155(4):517-31. [Crossref] [Google Scholar] [PubMed]
31. Sahoo RN, Satapathy BS, Ray J, Dash R, Mallick S. Celecoxib crystallized from hydrophilic polymeric solutions showed modified crystalline behavior with an improved dissolution profile. Assay Drug Dev Technol 2021;19(4):237-45.
32. Bhattacharya SS, Banerjee S, Chowdhury P, Ghosh A, Hegde RR, Mondal R. Tranexamic acid loaded gellan gum-based polymeric microbeads for controlled release: *In vitro* and *in vivo* assessment. Colloids Surf B Biointerfaces 2013;112:483-91.
33. Calvo P, Remunan-Lopez C, Vila-Jato JL, Alonso MJ. Novel hydrophilic chitosan-polyethylene oxide nanoparticles as protein carriers. J Appl Polym Sci 1997;63(1):125-32.
34. Danhier F, Lecouturier N, Vroman B, Jérôme C, Marchand-Brynaert J, Feron O, *et al.* Paclitaxel-loaded PEGylated PLGA-based nanoparticles: *in vitro* and *in vivo* evaluation. J Control Release 2009;133(1):11-7.
35. Balla A, Goli D. Formulation and evaluation of PLGA nanoparticles of ropinirole HCl for targeting brain. Indian J Pharm Sci 2020;82(4):622-31.
36. Chourasiya V, Bohrey S, Pandey A. Formulation, optimization, characterization and in-vitro drug release kinetics of atenolol loaded PLGA nanoparticles using 33 factorial design for oral delivery. Materials Discov 2016;5:1-3.
37. Roy A, Singh SK, Bajpai J, Bajpai AK. Controlled pesticide release from biodegradable polymers. Cent Eur J Chem 2014;12:453-69.
38. Grant GT, Morris ER, Rees DA, Smith PJ, Thom D. Biological interactions between polysaccharides and divalent cations: The egg-box model. FEBS let 1973;32(1):195-8.
39. Morris ER, Rees DA, Thom D, Boyd J. Chiroptical and stoichiometric evidence of a specific, primary dimerisation process in alginate gelation. Carbohydr Res 1978;66(1):145-54.
40. Halder A, Maiti S, Sa B. Entrapment efficiency and release characteristics of polyethyleneimine-treated or-untreated calcium alginate beads loaded with propranolol–resin complex. Int J Pharm 2005;302(1-2):84-94.
41. Jithendra P, Rajam AM, Kalaivani T, Mandal AB, Rose C. Preparation and characterization of aloe vera blended collagen-chitosan composite scaffold for tissue engineering applications. ACS Appl Mater Interfaces 2013;5(15):7291-8.
42. Nejatzadeh-Barandozi F, Enferadi ST. FT-IR study of the polysaccharides isolated from the skin juice, gel juice, and flower of Aloe vera tissues affected by fertilizer treatment. Org Med Chem Lett 2012;2:1-9. [
43. Ray A, Aswatha SM. An analysis of the influence of growth periods on physical appearance, and acemannan and elemental distribution of Aloe vera gel. Ind Crop Prod 2013;48:36-42.
44. Lim ZX, Cheong KY. Effects of drying temperature and ethanol concentration on bipolar switching characteristics of natural Aloe vera-based memory devices. Phys Chem Chem Phys 2015;17(40):26833-53.
45. Bawane S, Telrandhe R, Pande SD. Formulation and evaluation of oral fast dissolving film of bisoprolol fumarate. Int J Pharm Drug Anal 2018;6(2):105-15. Marshell J, Gunasekaran S. The infrared and Raman spectra of propranolol hydrochloride. Indian J Phys 1996;70B(6):505-11.
46. Avadi MR, Sadeghi AM, Mohammadpour N, Abedin S, Atyabi F, Dinarvand R, *et al.* Preparation and characterization of insulin nanoparticles using chitosan and Arabic gum with ionic gelation method. Nanomed Nanotechnol Biol Med 2010;6(1):58-63.
47. Cao L, Lu W, Mata A, Nishinari K, Fang Y. Egg-box model-based gelation of alginate and pectin: A review. Carbohydr Polym 2020;242:116389.
48. Arun Krishna K, Vishalakshi B. Gellan gum-based novel composite hydrogel: Evaluation as adsorbent for cationic dyes. J Appl Polym Sci 2017;134(47):45527.
49. Angadi SC, Manjeshwar LS, Aminabhavi TM. Interpenetrating polymer network blend microspheres of chitosan and hydroxyethyl cellulose for controlled release of isoniazid. Int J Biol Macromol 2010;47(2):171-9.
50. Sharma YR. Elementary organic spectroscopy. S. Chand Publishing; 2007.
51. Rao CNR. Chemical applications of spectroscopy. Academic Press, New York; 1963.
52. Novientri G, Abbas GH, Budianto E. Nanocomposite hydrogel-based biopolymer modified with silver nanoparticles as an antibacterial material for wound treatment. J Appl Pharm Sci 2019;9(11):001-9.
53. Greenstein PD, Casabianca LB. Interplay between π-stacking and hydrogen bonding in the self-association of different isomers of naphthalenedicarboxylic acid. J Phys Chem B 2017;121(19):5086-93.
54. Wang N, Cheng X, Li N, Wang H, Chen H. Nanocarriers and their loading strategies. Adv Healthc Mater 2019;8(6):1801002.
55. Liu J, Xiao J, Li F, Shi Y, Li D, Huang Q. Chitosan-sodium alginate nanoparticle as a delivery system for ε-polylysine: Preparation, characterization and antimicrobial activity. Food Control 2018;91:302-10.
56. Katuwavila NP, Perera AD, Samarakoon SR, Soysa P, Karunaratne V, Amaratunga GA, *et al.* Chitosan-alginate nanoparticle system efficiently delivers doxorubicin to MCF-7 cells. J Nanomater 2016;2016:3178904.
57. Costa P, Lobo JM. Modeling and comparison of dissolution profiles. Eur J Pharm Sci 2001;13(2):123-33.
58. Brahmankar DM, Jaiswal SB. Biopharmaceutics and pharmacokinetics: A treatise. Vallabh prakashan; 2015.